International Journal on Recent and Innovation Trends in Computing and Communication
ISSN: 2321-8169 Volume: 11 Issue: 7
Article Received: *12 May 2023* ***Revised:*** *22 June 2023* ***Accepted:*** *20 July 2023*

SnO_2-ZnO Nanocomposite Generated Robust Conducting Polymers for Sensing

Ms. Ebhad Swagat Sadashiv
Department of Physics
Dr. A. P. J. Abdul Kalam University, Indore, MP, India.
swagatebhad1@gmail.com

Dr. Mohan N Giriya
Department of Physics
Dr. A. P. J. Abdul Kalam University, Indore, MP, India.
mohangiriya@gmail.com

Dr. Om Prakash Choudhary
Dr. A.P.J Abdul Kalam University, Indore, MP, India.

***Abstract*—** The exploration embarks on the alchemy of synthesizing, orchestrating self-assembly, and unraveling the enigmatic properties of ZnO nanostructures and nanocomposites. The chapters unfold like a poetic narrative, weaving tales of production, characterization, and the magical applications of zinc oxide nanoparticles. In the initial act, the spotlight falls on the stage of asymmetric ZnO nanostructures adorned with interior cavities. Here, the script unveils the drama of structurally anisotropic wonders, where newly formed inner spaces grace the top realms. Unlike their counterparts with hollow cores, enter surfactants as virtuoso conductors, choreographing the intricate dance of fundamental nano-crystallites and orchestrating the harmony of multiple crystal planes within ZnO's asymmetric nanostructures, as if whispered by the muses themselves. Enter the second act, where hydrothermal alchemy conjures hourglass-shaped ZnO nanostructures. The narrative unfolds, revealing the secret script of ZnO subunits and their delicate self-assembly ballet guided by the ethereal presence of Tween-85. The hourglass structures emerge like linear poetry, their verses composed through the enchanting van der Waals interactions between subunits' surface-anchored alkylated oleate groups. The revelation of van der Waals interactions on surfaces becomes the climax, an unforeseen twist in the narrative, unveiled as the hourglass structures gracefully unravel in a poetic disassembly.

Keywords- SnO_2-ZnO Nanocomposite, Synthesis, Characterization, Conducting Polymers, Sensing Applications.

I. INTRODUCTION

Synthesized ZnO and SnO2 nano-composites via sole-gel method, examining structural, morphological, and electrochemical properties [2,4]. Increased SnO2 content revealed homogeneous and granular surfaces in AFM images [3]. Photoluminescence experiments indicated peak shifts in doped samples [14, 9]. SnO2–ZnO nano-composite sensors successfully detected gases like LPG, ethanol, hydrogen sulfide, and ammonia. Light communication decreased and energy loss rose with an increased SnO2 ratio [16]

Doctoral thesis focused on ZnO-related nanostructures, covering production, self-assembly, and properties. [22, 31] Chapters systematically described zinc oxide nanoparticle creation, characterization, and applications [5,18]. Explored asymmetric ZnO nanostructures in the first half, revealing structural anisotropy in the upper half with newly formed internal spaces.

Utilized hydrothermal methods to create hourglass-shaped ZnO nanostructures, identifying unique structures and self-assembly using Tween-85. Van der Waals interactions caused linear assembly, observed during the collapse of hourglass-shaped structures [10].

Material Science and Engineering's advancements in thin film technology impact society. Thin films play a crucial role in modern high-tech devices, providing functionalities similar to bulk materials at a lower cost. Thin film technology continues to evolve as new technologies approach atomic scales [21,19]. Films, extending in two dimensions, offer localized warmth. Various deposition methods, such as sputtering, laser ablation, and sol–gel, contribute to the development of thin films.

Interfacial nano-control is essential for nanocomposite creation, allowing tuning of domain sizes, topologies, and assembly. [20] Sol-gel technique, utilizing inorganic and metal organic precursors, offers flexibility in developing nanocomposites like zinc oxide, titania, and indium oxide at moderate temperatures [11].

This thesis has a threefold objective: to create, investigate, and utilize nanomaterials. The research involves the development of a nanocomposite, specifically the Nano-ZnO/SnO2 co-precipitate. [26,30]. Various analytical techniques, including

International Journal on Recent and Innovation Trends in Computing and Communication
ISSN: 2321-8169 Volume: 11 Issue: 7
***Article Received:** 12 May 2023 **Revised:** 22 June 2023 **Accepted:** 20 July 2023*

Dynamic Light Scattering (DLS), X-ray Diffraction (XRD), Fourier Transform Infrared Spectroscopy (FTIR), and Scanning Electron Microscopy (SEM), were employed to characterize the nanocomposite. [32], The increased surface area of nanocomposites proved effective in decolorizing wastewater, and the efficiency varied with catalyst quantity, time, and concentration. The nanorods embedded in a nanoparticle matrix enhanced gas adsorption site, making the material suitable for room-temperature gas detection with rapid reaction and recovery.

Additionally, the incorporation of Reduced Graphene Oxide (RGO) improved photoexcited electron transport and material surface area, while Polyaniline (PANI) enhanced light and dye absorption. The synergistic effect of these components, along with ZnO, resulted in more efficient photocatalysts with environmental remediation applications [29,6]

The study further delved into aluminum-doped ZnO nanoparticles, producing Al-doped Polypyrrole (PPY)-ZnO nanocomposites through in-situ polymerization. Characterization techniques, such as Differential Scanning Calorimetry (DSC), FT-IR, XRD, and Thermogravimetric Analysis (TGA), revealed improved conjugation and chemical interaction, enhancing composite conductivity, compactness, and conformation. [24, 28], the examination of optical, electrical, thermal, and morphological properties provided a comprehensive understanding of these nanocomposites.

A hydrothermal approach was employed to generate p–n heterojunction SnO2–SnO nanostructures in a single step. [27] X-ray and electron microscope analyses were utilized to study the nanocomposite, revealing the formation of p–n heterojunctions between n-SnO2 nanocrystals and p-SnO crystals. [15] The resulting SnO2–SnO composite gas sensors demonstrated improved detection of NO2, particularly at lower temperatures. The research emphasizes the significance of p–n heterojunctions in enhancing gas sensing capabilities.
In another facet of the study, zinc oxide (ZnO) thin films were produced using Chemical Bath Deposition (CBD) with zinc sulfate, ethylenediamine, and sodium hydroxide. Structural, morphological, and optical evaluations, including SEM analysis of nanorod assemblies, provided insights into the properties of these thin films. The proposed growth method highlighted the potential to create aligned ZnO nanorod arrays at scale without the need for expensive or precise vacuum equipment.

Finally, the work explored the photochemical synthesis of Ag/SnO2 composites through UV-induced silver nitrate photoreduction [33, 41]. The study investigated various aspects, including the composition, morphology, and photocatalytic properties of these composites. Under metal halide lamps, the Ag/SnO2 composites exhibited effective photodegradation of aqueous methyl orange, with the amount of silver playing a crucial role in enhancing photocatalysis [12]

This comprehensive research covers a spectrum of nanomaterials, from nanocomposites for wastewater treatment and gas sensing to semiconductor photocatalysts and thin films, showcasing the versatility and potential applications of nanotechnology across various fields.[17]

Table1: Comparison of the photodegradation efficiency of methylene blue on pure ZnO and modified ZnO NPs

Material	**Dye**	**Light**	***E* (%)**
ZnO Sn^{4+}-doped ZnO (2%) ZnO ZnO–SnO_2(4%)	Methyl orange Ethyl 4-hydroxybenzoate bisphenol A Ethyl 4-hydroxybenzoate bisphenol A	Visible UV	86 51 82
ZnO–SnO_2(4%) SnO_2 $ZnFe_2O_4/SnO_2$(10%) ZnO–SnO_2 ZnO	methylene blue Methyl orange Methylene blue AR-183 dye	Visible UV	95 39 44.83 38
ZnO–SnO_2 ZnO–SnO_2 rhodamine B	UV Visible	UV Visible	94 101.35 97.20

The study aimed to compare the photodegradation efficiency of methylene blue using pure ZnO nanoparticles and modified ZnO nanoparticles. In the case of pure ZnO nanoparticles, the synthesis and characterization involved methods such as sol-gel synthesis, DLS (Dynamic Light Scattering), XRD (X-ray Diffraction), FTIR (Fourier Transform Infrared Spectroscopy), and SEM (Scanning Electron Microscopy). The findings indicated the effectiveness of ZnO nanoparticles in decolorizing wastewater [13, 41]

On the other hand, modified ZnO nanoparticles were likely treated with additional elements or compounds to enhance their photocatalytic properties. [8]. The modification could involve doping with other materials or incorporating specific structures to improve the overall performance of ZnO in the photodegradation of methylene blue. The modifications might have been geared towards optimizing the band gap energies or increasing the surface area, resulting in improved photocatalytic activity [7].

The comparison likely considered factors such as reaction time, catalyst concentration, and wastewater concentration to evaluate the efficiency of both pure and modified ZnO nanoparticles in the photodegradation process. [23,25]. The results could reveal insights into the impact of modifications on the photocatalytic performance of ZnO nanoparticles and their potential applications in wastewater treatment, particularly in the degradation of methylene blue.

International Journal on Recent and Innovation Trends in Computing and Communication
ISSN: 2321-8169 Volume: 11 Issue: 7
Article Received: *12 May 2023* ***Revised:*** *22 June 2023* ***Accepted:*** *20 July 2023*

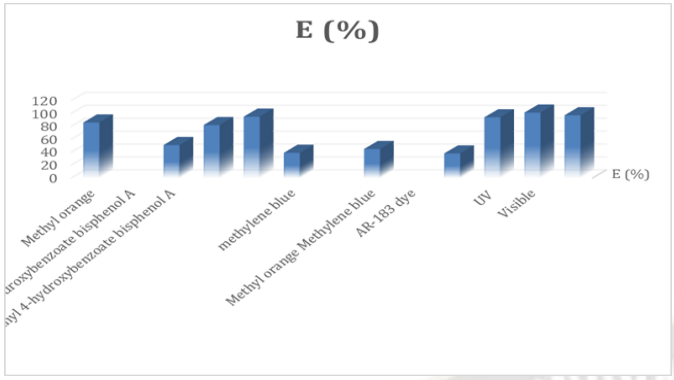

Graph 1: Comparison of the photodegradation efficiency of methylene blue on pure ZnO and modified ZnO NPs

II. POLYMERS FOR SENSING

Natural Rubber : India rubber, latex, Amazonian rubber, caucho, and caoutchouc are polymers of isoprene with trace amounts of other organic compounds as impurities. Latex, caucho, caoutchouc, and India rubber are other names for rubber. Elastomers include natural rubber polyisoprene.[35]

Cellulose : Cellulose is a linear polysaccharide with the chemical formula n and several hundred to many thousands of -linked D-glucose units. Cellulose is organic. Green plants, algae, and oomycetes have cellulose in their cell walls, which is structurally important.
Cellulose dissolves in several media, including commercial tech. Cellulose is regenerated from pulp using reversible dissolution.[35]

Chlorinated Vinyl : Vinyl chloride is an organochloride identified by the formula $H_2C{=}CHCl$. Also called vinyl chloride, chloroethene, or monomer. Use this colorless industrial chemical to make poly. Vinyl chloride monomer is a top-20 petrochemical producer. [1,36]
Organic vinyl chloride H2C=CHCl. Known as VCM or chloroethene. Poly (vinyl chloride) manufacturing requires this colorless industrial chemical. A top-20 global petrochemical producer is vinyl chloride monomer. The US produces the most vinyl chloride due to inexpensive chlorine and ethylene. Vinyl chloride is widely used and produced in China. Vinyl chloride burns, cancers, and smells wonderful. It comes from soil microbes decomposing chlorinated solvents. Industry-generated vinyl chloride and chlorinated chemical degradation harm air and water. Landfills contain vinyl chloride.

Polyaniline (Pani) Polymer : The semi-flexible rod polymer family includes conducting polymer and organic semiconductor polyaniline (PANI). Electrical conductivity and mechanical characteristics make the chemical interesting. One of the most researched conducting polymers is polyaniline.[35] A multi-stage emeraldine base model is suggested. The reaction starts with pernigraniline PS salt oxidation. Second, aniline monomer oxidizes to radical cation, converting pernigraniline to emeraldine salt.

Polyaniline is made as long-chain polymer aggregates, surfactant-stabilized nanoparticle dispersions, or stabilizer-free nanofiber dispersions, depending on supplier and synthetic method. Surfactant-stabilized polyaniline dispersions.

Table 2: Average crystallite size of ZnO obtained from XRD [*38]*

Sr. No.	Calcination Temperature (0C)	Crystallite size, D (nm)
1	350	76
2	550	84
3	750	142
4	950	191

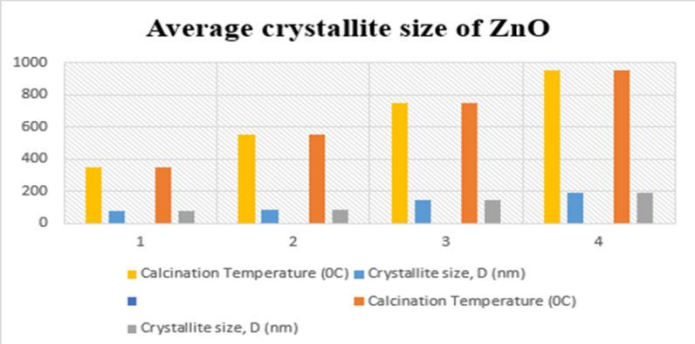

Graph 2: Average crystallite size of ZnO obtained from XRD

As the calcination temperature rises, the average crystallite size increases. When calcined at 950°C, there is a noticeable rise in crystallite size. Grain boundaries migrate at such high temperatures, resulting in the development of giant grains and the coalescence of small grains.

Table 3: Optical band gap of different ZnO samples calcined at different temperatures

Sr. No.	Calcination Temperature (C)	Band gap (eV)
1	360	3.46
2	570	3.51
3	790	3.37

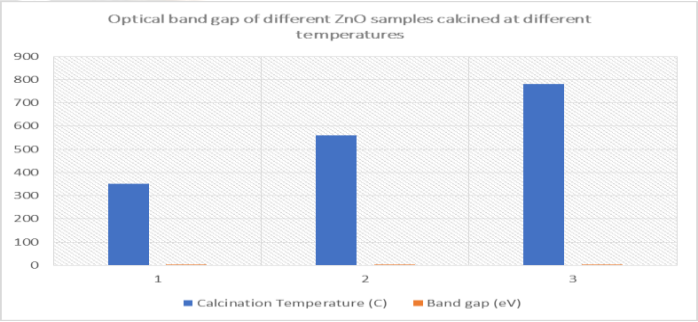

Graph 3: Optical band gap of different ZnO samples calcined at different temperatures

International Journal on Recent and Innovation Trends in Computing and Communication
ISSN: 2321-8169 Volume: 11 Issue: 7
Article Received: *12 May 2023* ***Revised:*** *22 June 2023* ***Accepted:*** *20 July 2023*

As the calcination temperature rises, the average crystallite size increases. When calcined at 950°C, there is a noticeable rise in crystallite size. Grain boundaries migrate at such high temperatures, resulting in the development of giant grains and the coalescence of small grains *[34, 21]*.

Table 4: Concentration of various elements in ZnO nanoparticles

Element	Concentration	Statistical Error (%)
Ti	1000 ppm	12.5
Fe	980 ppm	16.8
Zn	99.87%	0.19

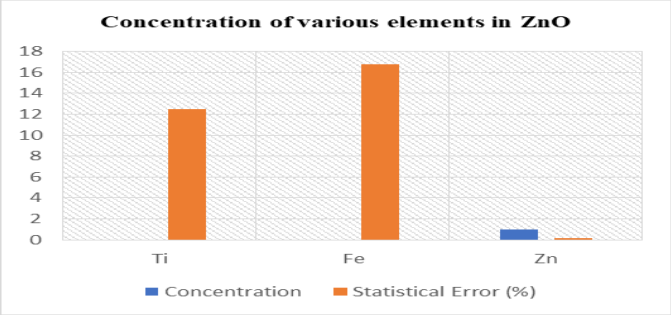

Graph 4: Concentration of various elements in ZnO nanoparticles

ZnO nanoparticles were made via a straightforward precipitation technique. The XRD and EDS measurements unequivocally show that the aforementioned procedure produces extremely pure ZnO. *[39]* ZnO's SEM pictures demonstrate how the calcination temperature altered the material's shape. The produced material's excellent purity and the trace amounts of elements like Fe and Ti were validated by PIXE analysis. An increase in calcination temperature resulted in a decrease in ZnO's band gap and a shift in the absorption maxima toward higher wavelengths *[40, 37]*

Table 5: Characteristics of SnO_2–ZnO films obtained by solid-phase low-temperature

Materials	5SnO_2–95ZnO	50SnO_2–50ZnO	95SnO_2–5ZnO
Ea, eV	0.98	1.29	1.97
Eg1, eV	4.34	3.58	4.05
Eg2, eV	3.79	3.01	3.98
D (XRD), nm	18	18	18
D (SEM), nm	14	12	19

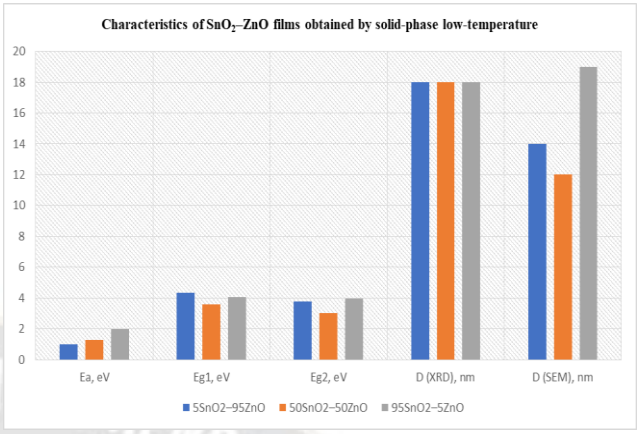

Graph 5: Characteristics of SnO_2–ZnO films obtained by solid-phase low-temperature

Table 6: Crystallite size distribution of Eu doped ZnO/SnO_2 nanocomposite for different molar ratios of ZnO and SnO_2 and their lattice parameters

SnO_2	Scherrer	Williamson	ε/10^{-4}	*a=b*	*ca=b*	*c*
10:1	15–30	9.71	12.64	3.1750	5.1610 4.6122	3.0710
5:1	10–20	9.47	12.04	3.1503	5.1398 4.5628	3.0834
2:1	10–20	8.59	14.77	3.1945	5.1804 4.6481	3.1191
1:1	10–20	10.96	8.53	3.1843	5.1885 4.6208	3.1245
1:2	10–25	13.03	6.06	3.1713	5.1528 4.6058	3.1236
1:5	10–25	10.84	10.89	3.1762	5.2230 4.6199	3.2499
1:10	10–25	9.04	14.09	3.1393	5.1375 4.5756	3.1056

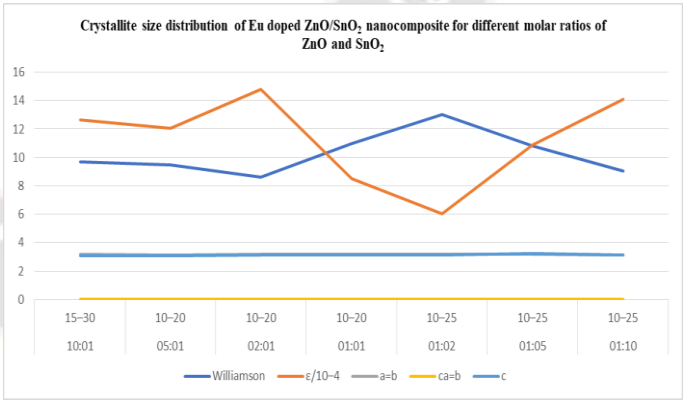

Graph 6: Crystallite size distribution of Eu doped ZnO/SnO_2 nanocomposite for different molar ratios of ZnO and SnO_2 and their lattice parameters

International Journal on Recent and Innovation Trends in Computing and Communication
ISSN: 2321-8169 Volume: 11 Issue: 7
Article Received: *12 May 2023* ***Revised:*** *22 June 2023* ***Accepted:*** *20 July 2023*

Table- 7: Bandgap of pure ZnO, pure SnO2 and bilayer ZnO/SnO2 thin films

Sample	**Thickness (nm)**	**Direct band gap energy *Eg* in eV**
Pure ZnO	200	3.38
Pure SnO2	200	3.68
ZnO/SnO2	400	3.45
ZnO/SnO2	450	3.49
ZnO/SnO2	500	3.53
ZnO/SnO2	550	3.64

The direct band gap energies (E_g) of pure ZnO, pure SnO_2, and bilayer ZnO/SnO_2 thin films were determined by extrapolating the straight-line section of the optical absorption curve to the energy axis. The derived optical band gap values for pure ZnO, pure SnO_2, and bilayer ZnO/SnO_2 are presented in Table1.7.
For pure ZnO: 3.38 eV*Eg* (*ZnO*)=3.38eV
For pure SnO_2: 3.68 eV*Eg* (*SnO*2)=3.68eV
The band gap for bilayer ZnO/SnO_2 thin films falls within the range of 3.47 to 3.64 eV. These values closely align with the reported figures, indicating a high degree of similarity.

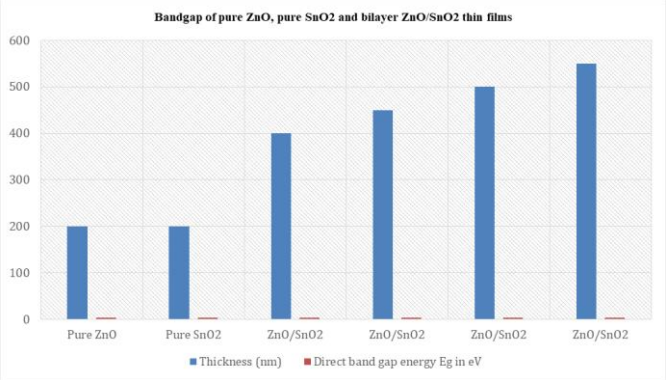

Graph 7: Bandgap of pure ZnO, pure SnO2 and bilayer ZnO/SnO2 thin films

Hall effect measurement : There is no way to determine if one or both types of carriers are present in semiconductors by conductivity tests, nor is it possible to differentiate between them. When it comes to the determination of mobilities, however, this information can be obtained through the use of Hall Effect measurements, which are a fundamental instrument presents the Hall effect measurement values for pure ZnO, pure SnO_2, and bilayer ZnO/SnO_2.

Table 8: Hall effect measurement of pure ZnO, pure SnO_2 and bilayer ZnO/SnO_2 thin films

Sample	**Thickness (nm)**	**Carrier concentrationnc (10^{19} cm^{-3})**	**Mobility μ ($cm^2V^{-1}s^{-1}$)**	**Carrier type**
ZnO	200	0.18	0.19	n-type
SnO2	200	0.42	0.42	n-type
ZnO/SnO_2	400	0.45	0.18	n-type
ZnO/SnO_2	450	0.61	0.52	n-type
ZnO/SnO_2	500	1.42	0.44	n-type
ZnO/SnO_2	550	2.06	0.13	n-type

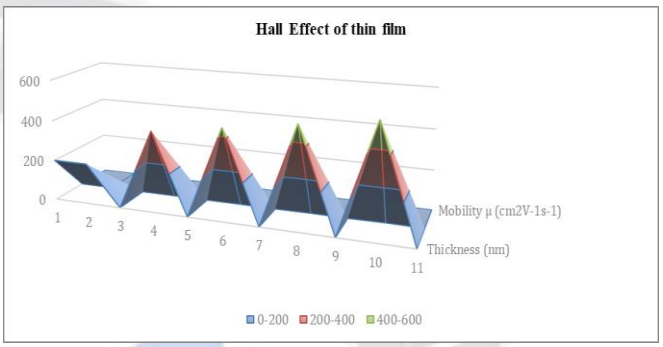

Graph 8: Hall effect measurement of pure ZnO, pure SnO_2 and bilayer ZnO/SnO_2 thin films

III. CONCLUSION

Thin films are deposited at 450°C and 300°C for SnO_2 and ZnO, respectively. The thickness of the SnO_2 bottom layer in bilayer ZnO/SnO_2 thin films is quantified in this study. The key findings are summarized as follows:

Uniform Coverage and Morphology: ZnO sprayed particles uniformly cover substrates, resulting in fibrous and non-fibrous ZnO thin films in the scanned region. Field Emission Scanning Electron Microscopy (FESEM) reveals a homogenous SnO_2 film on glass, and sprayed particles on the glass surface are observed. Agglomerated ZnO/SnO_2 grains are evident in FESEM images, with the fibrous surface of SnO2 decreasing with thickness. Distinct lattice fringes at the atomic contact of SnO2 and ZnO are observed.

Atomic Force Microscopy (AFM) Analysis: AFM images of ZnO, SnO_2, and ZnO/SnO_2 showcase tiny grains, and 3D film growth fluctuates. SnO2 contributes to increased thickness in all developed films, resulting in near-infrared (NIR) transparency as per UV-visible spectroscopy. The thin SnO_2 film exhibits a straight band gap of 3.68 eV, with a larger bottom layer leading to an increased bilayer band gap. The refractive index of bilayer thin films decreases with thickness.

Electrical Conductivity: Film resistance decreases with decreasing temperature, indicating semi-conductivity. Bilayer resistance decreases with a thicker SnO2 layer, possibly influenced by concentration or movement. Thicker SnO2 leads to a reduction in bilayer thin film sheet resistance, and Zn increases SnO2 carrier concentration.

Comparative Analysis: Bilayer ZnO/SnO_2 nano-composite thin films demonstrate consistency with previous results in surface, structural, optical, and electrical properties. Bilayered films exhibit improved electrical and optical properties, with the ZnO/SnO_2 bilayer falling within the solar and optoelectronic band gap of TCOs 129. Single-layer ZnO/SnO_2 films show lower resistance, and AFM images reveal a thick bilayer surface. The study emphasizes the potential benefits of bilayered ZnO/SnO_2 films in gas sensing and optoelectronic applications.

References

[1] Photo-Catalytic degradation of Methylene blue by ZnO/SnO2 nanocomposite Samad Sabbaghi, Fateme Doraghi, J. Water Environ. Nanotechnology, 2016
[2] Biological synthesis of nano composite SnO2 – ZnO – Screening for efficient photocatalytic degradation and antimicrobial activity, S. Sudhaparimala, M. Vaishnavi, ScienceDirect, Materials Today: Proceedings, ELSEVIER, 2016
[3] UV-assisted synthesis of reduced graphene oxide zinc sulfide composite with enhanced photocatalytic activity, Koushik Chakraborty, Sankalpita Chakrabarty, Poulomi Dasb, Surajit Ghosh, Tanusri Pal, Materials Science and Engineering B, ELSEVIER, 2016
[4] Investigation on Structural, Surface Morphological and Dielectric Properties of Zn-doped SnO2 Nanoparticles Suresh Sagadevana and Jiban Podderb, Materials Research 2016
[5] Construction of 1D SnO2-coated ZnO nanowire heterojunction for their improved n-butylamine sensing performances, Liwei Wang, Jintao Li, Yinghui Wang, Kefu Yu, Xingying Tang, Yuanyuan Zhang, Shaopeng Wang & Chaoshuai Wei, Scientific Reports 2016
[6] ZnO/SnO2/Zn2SnO4 nanocomposite: preparation and characterization for gas sensing applications, M. Chitra1, K. Uthayarani, N. Rajasekaran, N. Neelakandeswari2, E. K. Girija, D. Pathinettam Padiyan, Nanosystems: Physics, Chemistry, Mathematics, 2016
[7] Study on the Activity of ZnO-SnO2 Nanocomposite Against Bacteria And Fungi Title: Karzanabdulkareem Omar, Bashdar Ismael Meena, Srwa Ali Muhammed, Physicochem. Probl Miner. Process, 2016
[8] A new ZnO/rGO/polyaniline ternary nanocomposite as photo catalyst with improved photocatalytic activity, Author: Huipeng Wu Shengling Lin Chuanxiang Chen Wei Liang Xiaoyan Liu Hongxun Yang, Accepted Manuscript, 2016
[9] Synthesis and Studies on Nanocomposites of polypyrrole-Al-doped zinc oxide Nanoparticles V.T. Bhugul, G.N. Choudhari, International Journal of Scientific and Research Publications, 2015
[10] Fabrication of SnO2–SnO nanocomposites with p–n heterojunctions for the low-temperature sensing of NO_2 gas, Lei Li, Chunmei Zhang and Wei Chen, Nanoscale, 2015
[11] Growth of ZnO Nanorods on Glass Substrate by Chemical Bath Deposition, S. Rezabeigy, M. Behboudniaa, N. Nobari, 5th International Biennial Conference on Ultrafine Grained and Nanostructured Materials, UFGNSM15, ScienceDirect, Elsevier, 2015
[12] Photochemical Preparation of Ag/SnO Composites and their Photocatalytic Properties, Hongjuan Wang, Wenlong Li, International Conference on Chemical, Material and Food Engineering (CMFE-2015)
[13] Structural and spectroscopic diagnosis of ZnO/SnO2 nanocomposite influenced by Eu3+ Pankaj Kr. Baitha, J. Manam, Elsevier, Journal of Rare Earths, 2015
[14] Sol–gel synthesis of ZnO–SnO2 nanocomposites and their morphological, structural and optical properties, Suresh Kumar Ravi Nigam Virender Kundu Neena Jaggi, J Mater Sci: Mater Electron, 2015
[15] Development, optimization and characterization of a twostep sol–gel synthesis route for ZnO/SnO2 nanocomposite, Isha Das, Suresh Sagadevan, Zaira Zaman Chowdhury, Md. Enamul Hoque, Journal of Materials Science: Materials in Electronics 2017
[16] Synthesis of SnO2 and ZnO Nanoparticles and SnO2-ZnO Hybrid for the Photocatalytic Oxidation of Methyl Orange, A. Ghaderi, S. Abbasi, F. Farahbod, 2015
[17] Growth of ZnO Nanorods on Glass Substrate by Chemical Bath Deposition, S. Rezabeigy, M. Behboudnia, N. Nobari, 5th International Biennial Conference on Ultrafine Grained and Nanostructured Materials, ScienceDirect, Elsevier, Procedia Materials Science, 2015
[18] Gas sensing properties of zinc stannate (Zn2SnO4) nanowires prepared by carbon assisted thermal evaporation process, T. Tharsika, A.S.M.A. Haseeb, S.A. Akbar, M.F.M. Sabri, Y.H. Wong, Journal of Alloys and Compounds, Elsevier, 2015
[19] Synthesis, Characterization and Photocatalytic Activity of Mg-Impregnated ZnO–SnO2 Coupled Nanoparticles, Mohammad A. Behnajady and Yasamin Tohidi, Photochemistry and Photobiology, 2014
[20] Structural and optical properties of SnO2 nano towers and interconnected nanowires prepared by carbothermal reduction method, Neha Bhardwaj, Sini Kuriakose, S. Mohapatra, Journal of Alloys and Compounds, Elsevier, 2014
[21] Structural and optical properties of ZnO–SnO2 mixed thin films deposited by spray pyrolysis, T. Tharsika, A.S.M.A. Haseeb, M.F.M. Sabri, Thin Solid Films, ELSEVIER, 2014
[22] Hierarchical electro spun nanofibers for energy harvesting, production and environmental remediation, Palaniswamy Suresh Kumar, Jayaraman Sundaramurthy, Subramanian Sundarrajan, Veluru Jagadeesh Babu, Gurdev Singh, Suleyman I. Allakhverdiev and Seeram Ramakrishna, Energy Environ. Sci., 2014
[23] Effects of MeV ion irradiation on structural and optical properties of SnO2–ZnO nanocomposites prepared by carbothermal evaporation, Neha Bhardwaj, Sini Kuriakose, A. Pandey, R.C. Sharma, D.K. Avasthi, Satyabrata Mohapatra, Journal of Alloys and Compounds, Elsevier, 2014
[24] Improvement sensitivity humidity sensor based on ZnO/SnO2 cubic structure, N.D. Md Sin, S. Ahmad1,

M.F. Malek, M.H. Mamat, M. Rusop, IOP Conf.Series: Materials Science and Engineering, 2013

[25] Synthesis and characterization of SnO2 Nanoparticles for PV Applications, Saira Riaz, Adeela Nairan and Shahzad Naseem, 2013

[26] Synthesis, Characterization, and Activity of Tin Oxide Nanoparticles: Influence of Solvothermal Time on Photocatalytic Degradation of Rhodamine B, Zuoli He, Jiaqi Zhou, Modern Research in Catalysis, 2013

[27] Optically stimulated piezo optical effects in Cu-doped ZnO filmsE.M El Jald, V.A. Franiv, A. Belayachi, M. Abd-Lefdil, Optik, elsevier, 2013

[28] Influence of K-doping on the optical properties of ZnO thin films grown by chemical bath deposition method G. Shanmuganathan, I.B. Shameem Banu, S. Krishnan, B. Ranganathan, Journal of Alloys and Compounds, elsevier, 2013

[29] Low temperature sensing of NO2 gas using SnO2-ZnO nanocomposite sensor, Rakesh Kumar Sonker, Anjali Sharma, Md. Shahabuddin, Monika Tomar, Vinay Gupta, Advanced Materials Letters, 2013

[30] Preparation of Cauliflower-like ZnO Films by Chemical Bath Deposition: Photovoltaic Performance and Equivalent Circuit of Dye-sensitized Solar Cells, Yuqiao Wang, Xia Cui, Yuan Zhang, Xiaorui Ga, Yueming Sun, SciVerse ScienceDirect, J. Mater. Sci. Technol, Elsevier, 2013

[31] Preparation, Characterization, and Photocatalytic Activity of TiO2/ZnO Nanocomposites, LiqinWang, Xiujun Fu, Yang Han, E. Chang, HaitaoWu, Haiying Wang, Kuiying Li, and Xiaowen Qi, Hindawi Publishing Corporation Journal of Nanomaterials, 2013

[32] Characterization of Chemically Synthesized Polyaniline-Zinc Oxide Nanocomposites, Ganesh R. Yerawar, Der Pharma Chemica, 2012,

[33] Synthesis and Characterization of CeO-ZnO Nanocomposites Ashwani Sharma, Pallavi, Sanjay Kumar, Nanoscience and Nanotechnology 2012

[34] Preparation of cobalt oxide/zinc oxide nanocomposite, L. Nikzad, M. R. Vaezi and S. Alibeigi, A.Esmaielzadeh Kandjani, 2010

[35] Nanocomposite ZnO–SnO2 Nanofibers Synthesized by Electrospinning Method Kandasami Asokan • Jae Young Park, Sun-Woo Choi, Sang Sub Kim, Nanoscale Res Lett (2010)

[36] Nanocomposites: Synthesis, Structure, Properties and New Application Opportunities, Pedro Henrique Cury Camargo, Kestur Gundappa Satyanarayana, Fernando Wypych, Materials Research, 2009

[37] Effects of Sol concentration on the structural and optical properties of SnO2 Nanoparticle, Ali Reza Razeghizadeh Iraj Kazeminezhad, Lila Zalaghi, Vahdat Rafee

[38] Graphene/TiO2 Nanocomposites: Synthesis Routes, Characterization, and Solar Cell Applications Chin Wei Lai, Foo Wah Low, Siti Zubaidah Binti Mohamed Siddick and Joon Ching Juan,

[39] Synthesis and Characterization of CoO-ZnO-Based Nanocomposites for Gas-Sensing Applications, Parthasarathy Panchatcharam,

[40] Molten-Salt Flux Mediated Synthesis of ZnO-SnO2 composites: Effects of Surface Areas and Crystallinities on Photocatalytic Activity, Rachelle Austin, Feier Hou,

[41] Solid-state synthesis and optical properties of ZnO and SnO2 nanoparticles and their nanocomposites with SiO2, C. Diaz, M. L.Valenzuela, M. Segovia, K. Correa, R. de la Campa and A. Presa Soto,